PERGAMON

Vision Research 42 (2002) 1837–1846

Vision Research

www.elsevier.com/locate/visres

Spatial frequency discrimination in cyclopean vision

P.M. Grove [a,1], D. Regan [a,b,*]

[a] Department of Psychology, York University, BSB room 375, 4700 Keele St., North York, Ont., Canada M3J 1P3
[b] Department of Biology, York University, BSB room 275, 4700 Keele St., North York, Ont., Canada M3J 1P3

Received 23 January 2002; received in revised form 24 April 2002

Abstract

It is well known that inspecting a cyclopean grating causes threshold for detecting a subsequently presented test cyclopean grating to be elevated, and that the threshold elevation is greatest at the adapting frequency. We report here that spatial frequency discrimination threshold is also elevated, but the elevation is greatest at frequencies offset from the adapting frequency, and the elevation at the adapting frequency is near-zero. We conclude that discrimination threshold is determined by the relative activity of cyclopean frequency-tuned channels, and suggest that relative activity is computed at an opponent-frequency stage. Discrimination threshold for cyclopean gratings was 2.5–4% for two observers, and remained approximately constant over the range 0.16–2.0 cycles/°. Discrimination threshold for luminance-defined gratings was only slightly lower. Discrimination threshold was approximately independent of the grating's peak-to-peak disparity over a range of 45:1 for one observer and 17:1 for another. This finding as well as the low value of discrimination threshold are consistent with an opponent-process model. The dot density of every cyclopean grating used was chosen bearing in mind our finding that three or more spatial samples per grating cycle are required before sampling effects can be ignored.

Keywords: Cyclopean; Spatial vision; Spatial discrimination; Sampling

1. Introduction

Although the vivid depth created by a stereoviewer was commonly attributed to binocular disparity in the years following Wheatstone (1838) paper, the stereo line drawings that he used contained monocular as well as binocular cues to depth, as do almost all stereo photographs. A demonstration that binocular disparity alone can support the perception of spatial form by breaking camouflage was not available until Julesz isolated neural processing that occurs after signals from the left and right eyes have converged. He did this by creating patterns that contain no monocularly-available cues to the camouflaged form (Julesz, 1960). A Julesz random dot stereogram consists of randomly located texture elements such as dots. One eye views such a pattern that is identical to the pattern viewed by the other eye except that one or more parts of the pattern are shifted bodily to the left or right. The resulting empty areas are filled in with more random dots. In monocular view the shifted area(s) are perfectly camouflaged: each pattern looks like a flat array of random dots. In binocularly-fused vision, however, normally sighted individuals see the camouflaged form. Furthermore, the camouflaged form is perceived in vivid depth. Many dramatic illustrations are to be found in Julsez (1971). Julesz called this kind of vision *cyclopean* and the kind of form seen in random dot stereograms *cyclopean form*. [2] The spatial properties of cyclopean perception have been recently reviewed (Regan, 2000, pp. 343–374).

* Corresponding author. Address: Department of Psychology, York University, BSB room 375, 4700 Keele St., North York, Ont., Canada M3J 1P3. Tel.: +1-416-736-5627; fax: +1-416-736-5814.
E-mail address: dregan@yorku.ca (D. Regan).
[1] Present address: School of Psychology, University of New South Wales, P.O. Box 1, Sydney, NSW 2052, Australia.

[2] The fact that a particular observer can see and recognize a cyclopean form does not, as is sometimes claimed, necessarily imply that the observer's visual system contains a mechanism sensitive to binocular disparity, though it does indicate that the observer's visual system contains a binocularly-driven mechanism. This point can be demonstrated by viewing a cyclopean target generated by the red–green analglyph technique. First, one observes that the hidden form is seen in vivid depth, but cannot be seen when one eye is closed. Now

0042-6989/02/$ - see front matter
PII: S0042-6989(02)00104-9

The contrast sensitivity curve for cyclopean gratings has been reported to be U-shaped with a peak sensitivity at ≈0.3 cycles/°, and a grating acuity of only ≈4 cycles/° (Rogers & Graham, 1985; Tyler, 1974). Evidence has been reported that this curve does not characterize a single psychophysical cyclopean channel. Rather, grating corrugations are processed through a parallel array of channels, each of which responds to only part of the spatial frequency range of the cyclopean contrast sensitivity curve (Cobo-Lewis & Yeh, 1994; Julesz & Miller, 1975; Schumer & Ganz, 1979; Tyler, 1975, 1983). Evaluating the conflicting estimates of cyclopean channel bandwidth, Howard and Rogers (1995, pp. 165–166) stated that the narrowest estimate of ≈1 octave (Tyler, 1983) was based on a masking technique which underestimates bandwidth because of "off channel looking", while the widest (≈2 octaves) estimates were based on procedures that were not subject to this criticism (e.g. Cobo-Lewis & Yeh, 1994; Schumer & Ganz, 1979).

Even though the widest estimate of channel bandwidth for cyclopean form is considerably wider than channel bandwidth for luminance-defined form (Campbell & Robson, 1968; Graham & Nachmias, 1971; Graham, 1989; Smallman, MacLeod, He, & Kentridge, 1996), the boundaries of a cyclopean target can appear to be remarkably sharp-considerably sharper than the boundaries of a luminance-defined target of matched spatial sampling (Regan & Hamstra, 1994, Fig. 2). By measuring discrimination for the relative position of cyclopean bars, Morgan (1986) showed that this perceived sharpness is not merely an illusion. He found that vernier step acuity for a cyclopean target was 40″, and that this was similar to vernier step acuity for a luminance-defined target with matched spatial sampling. Comparisons of discrimination threshold for cyclopean and luminance-defined form have also been reported for several other kinds of spatial discrimination. Bar separation discrimination thresholds have been reported to be little different for cyclopean and luminance-defined bars of matched spatial sampling (Kohly & Regan, 2001). Aspect-ratio discrimination threshold for cyclopean rectangles is little inferior to aspect-ratio discrimination for luminance-defined rectangle of matched spatial sampling (Regan & Hamstra, 1994). And orientation discriminations threshold for a cyclopean bar is similar to that for a luminance-defined bar of matched spatial sampling (Hamstra & Regan, 1995).

The existence of a tilt aftereffect for cyclopean form provides evidence that cyclopean channels are tuned to orientation as well as spatial frequency (Cavanagh, 1989; Tyler, 1975). With this in mind it has been proposed that the reason why orientation discrimination threshold for cyclopean form (as low as 0.6°) is considerably lower than even the orientation tuning bandwidth of channels for luminance-defined form is that orientation discrimination threshold for cyclopean form is determined by the pattern of activity among orientation-tuned channels for cyclopean form (Hamstra & Regan, 1995).

In this paper we compare spatial frequency discrimination thresholds for cyclopean gratings and for luminance-defined gratings of matched spatial sampling. To anticipate, we report that discrimination thresholds are little different for the two kinds of form and that discrimination threshold for cyclopean gratings is considerably less than the cyclopean channel bandwidth. This last finding can be understood in terms of evidence reported below that discrimination threshold is determined by the pattern of activity among cyclopean channels that are tuned to spatial frequency.

2. General methods

2.1. Apparatus

Cyclopean stimuli were generated on a PC that contained three 16 bit D/A converters, one for the x-axis, one for the y-axis and one for dot luminance (z-axis) (Cambridge Instruments model D300) and were displayed on a large-screen, electrostatically driven monitor (Hewlett–Packard model 1321A) with green P31 phosphor. This arrangement gave a maximum of ≈65,000 × 65,000 (i.e. 4×10^9) possible dot locations within the display. Each dot subtended 6′ at a viewing distance of 114 cm. The monitor was viewed through a pair of highspeed goggles (Cambridge Instruments model FE-1).

The display consisted of bright dots on a dark background. The dots could be arranged either quasi-randomly or in parallel rows and columns. The quasi-random arrangement was achieved as follows. The display was divided into N imaginary squares, where N was the number of dots. Each imaginary square contained one dot. Within any given imaginary square the dot was randomly assigned to one of the many possible

remove the red–green goggles. The shape is immediately visible. The same point can be made by progressively increasing the relative disparity of a cyclopean target to a point when the target can no longer be fused, then increasing the disparity further. Two copies of the target can be seen, but the target is not seen in depth. Orientation discrimination can be carried out for such an unfused cyclopean bar target (Hamstra & Regan, 1995), and aspect ratio discrimination can be carried out for such an unfused rectangular target (Regan & Hamstra, 1994). This calls into question the claim that disparity information is processed before form information (Julsez, 1971). Furthermore, if binocularly-driven neurons "speak to" disparity-sensitive neurons, then the so-called correspondence problem (faced by disparity sensitive neurons in their attempts to distinguish incorrect matches from correct matches) might be considerably more straightforward that often assumed, because the binocularly-driven neurons sense the presence location and shape of the cyclopean form without any computation of disparity.

locations within the imaginary square. For example, for a 1000-dot display, there were $\approx 4 \times 10^6$ possible locations within any given imaginary square.

A cyclopean grating was created in the conventional manner (Tyler, 1975). Relative disparity could be varied in increments of $\approx(65{,}000)^{-1}$ of the width of the display. All gratings were horizontal, because sinusoidal cyclopean gratings of any orientation other than horizontal contain monocular cues to grating periodicity, i.e. they are not truly cyclopean. (This is not the case for squarewave gratings.) Luminance gratings were created by setting peak-to-trough disparity to zero and impressing a sinusoidal variation of luminance on the dots.

2.2. Experimental design

We designed the stimulus set to check that observers based their responses on the task-relevant variable, and to measure the extent to which they were affected by the following three task-irrelevent variables: (1) variations of the perceived magnitude of depth corrugations (or of luminance contrast) caused by trial-to-trial variations in grating spatial frequency; (2) the distance between a bar of the grating and some fixed feature, such as the edge of the display; (3) any interaction between the grating's periodicity and the number of samples (i.e. dots) in the display. Except when stated otherwise the design was as follows. There were eight values of spatial frequency, eight values of peak-to-trough disparity, eight equally-spaced values of grating spatial phase, and eight values of the total number of dots. The maximum percentage variation in the total number of dots was set so that the maximum percentage variation in the mean number of dots along a line perpendicular to the grating's bars was equal to the maximum percentage variation in the grating's spatial frequency. The set of 192 stimuli consisted of combinations of the 32 possible values, and was divided into three subsets. Each subset can be visualized as an 8×8 square array. In the first subset the grating's spatial frequency and its peak-to-trough disparity were orthogonal. This can be visualized as follows: along the horizontal axis of the square array spatial frequency varied, but peak-to-trough disparity was constant, while the converse was true for the vertical axis of the array. For each of the 64 stimuli in the array a phase was assigned randomly from the eight possible values and a number of dots from the eight possible values of dot number. In the second 8×8 array, the grating's spatial frequency and phase were orthogonal, and peak-to-trough disparity and number of dots were assigned randomly from the possible values. In the third 8×8 array, the grating's spatial frequency and the number of dots were orthogonal, and peak-to-trough disparity and phase were assigned randomly from the possible values. In any given run the 192 stimuli were presented in random order. The stimulus organization just described ensured that observers could not know to which of the three arrays any given stimulus belonged. Observers were instructed to signal whether the grating last presented had a higher or lower spatial frequency than the mean of the stimulus set. The grating was visible until the observer responded (self-paced). Following the response the screen remained blank for 1.5 s in order to minimize adaptation.

2.3. Analysis of data

The percentage of "spatial frequency higher than the mean" was plotted versus grating spatial frequency and Probit analysis (Finney, 1971) was used to estimate spatial frequency discrimination threshold, defined as equal to $100\{0.5[(SF_{TEST})_{75} - (SF_{TEST})_{25}]\}/SF_{MEAN}$ where $(SF_{TEST})_{75}$ and $(SF_{TEST})_{25}$ were, respectively, the grating spatial frequencies that gave 75% and 25% "higher than the mean" responses and SF_{MEAN} was the mean spatial frequency of the stimulus set.

To check that observers ignored trial-to-trial variations in the grating's peak-to-trough disparity and spatial phase as well as the total number of dots, response data were plotted versus these three task-irrelevent variables as well as versus the task-relevent variable.

2.4. Observers

Observer 1 (PMG) was male, aged 33 years. Observer 2 was male, aged 30 years. Observers 3 and 4 were female, aged 18 and 33 years respectively. Observers 2–4 were naïve as to the aims of the study.

3. Experiment 1

3.1. Purpose

The aim of Experiment 1 was to find the number of spatial samples (dots) per cycle of the cyclopean grating above which the effect of spatial sampling on spatial frequency discrimination can be ignored.

3.2. Methods

At the viewing distance of 114 cm the display subtended 15° (horizontal) × 15°. The mean number of cycles across the display was 9, and mean spatial frequency was 0.58 cycles/°. The mean number of dots seen by each eye ranged from 90 to 7100. A complete stereopair was displayed every 27 ms for 90 dots, and every 29 ms for 7100 dots. Spatial frequency discrimination threshold was measured as a function of the mean

number of dots for both the quasi-random and the non-random arrangements of dots.

3.3. Observers

Observers 1 and 4 carried out Experiment 1.

3.4. Results

Fig. 1A–H shows data that were typical of the situation that the pattern contained sufficient dots to ensure a low discrimination threshold. Each run yielded three plots of response probability vs. spatial frequency. As would be expected if the observer's criterion was the

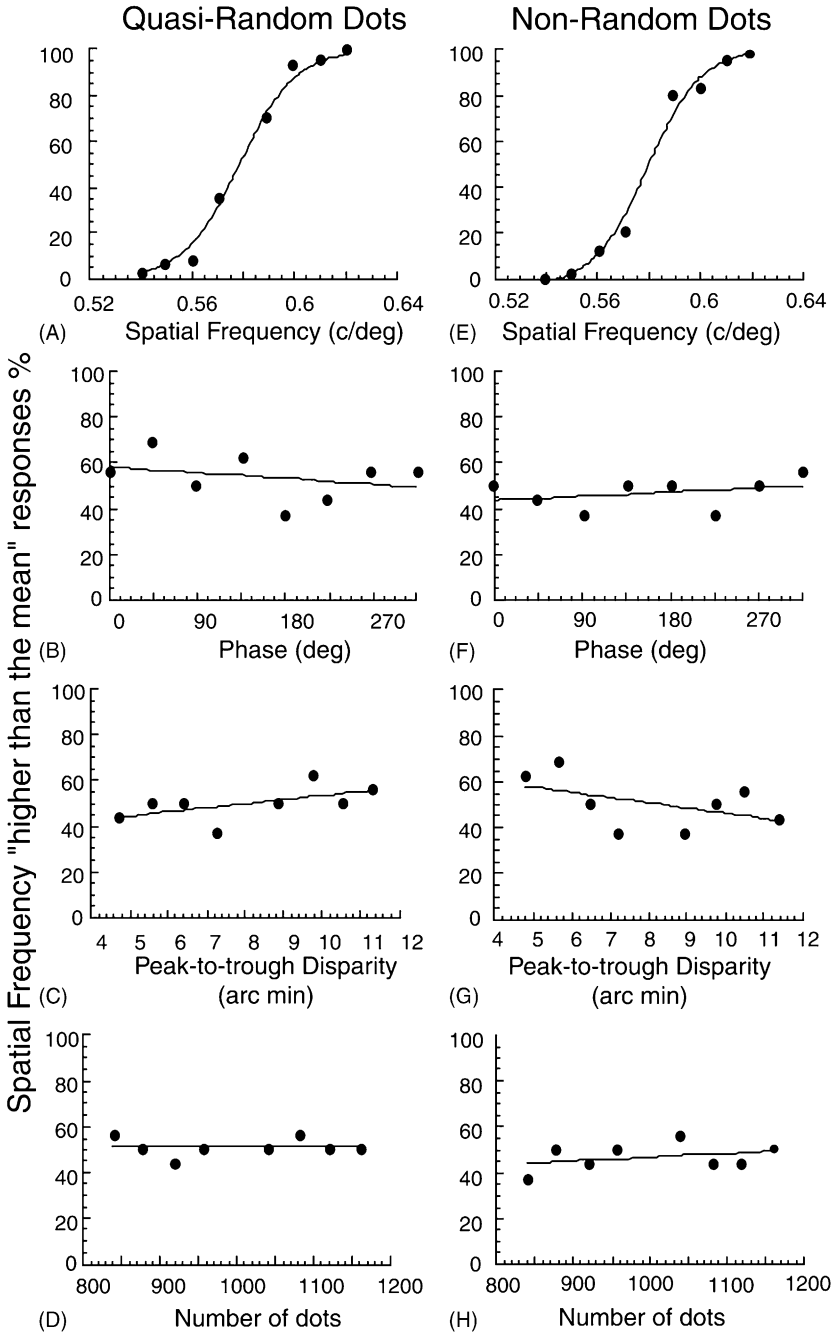

Fig. 1. Spatial frequency discrimination for cyclopean gratings in a quasi-random pattern of dots (A–D) and in a non-random pattern of dots (E–H). The percentage of "spatial frequency higher than the mean of the stimulus set" response was plotted versus the spatial frequency of the test grating (the task-relevant variable) in panels A and E, versus the spatial phase of the test grating (task-irrelevant variable no. 1) in panels B and F, versus the peak-to-trough disparity of the test grating (task-irrelevant variable no. 2) in panels C and G, and versus the total number of dots in the pattern (task-irrelevant variable no. 3) in panels D and H. The mean number of dots was 1000, giving three dots per grating cycle along a line at right angles to the bars of the grating. Observer 1.

same for each of the three stimulus subsets, the estimate of threshold was the same for each of the three plots. In Fig. 1A the three subsets of data have been combined and Fig. 1E was generated similarly. Fig. 1A–D and E–H shows that the responses of observer 1 were based on the task-relevant variable: the Fig. 1A plot was steep while the Fig. 1B–D plots were flat, and the Fig. 1E plot was steep while the Fig. 1F–H plots were flat. This steep/flat dichotomy indicated that the observer's responses were strongly influenced by the task-relevant variable while he ignored trial-to-trial variations in all three co-varying task-irrelevant variables. We confirmed that this was the case for both observers when the mean number of dots in the display totalled 1000 or more. When the total number of dots was progressively reduced below ≈1000 a pattern of results different to that shown in Fig. 1A–H was obtained. In particular the slopes in panels A and E were reduced (corresponding to an increase of threshold) and the slope in one or more of the other panels was increased (indicating that a task-irrelevant variable influenced the observer's responses).

In Fig. 2A and B the reciprocal of spatial frequency discrimination threshold was plotted as ordinate vs. the mean number of spatial samples per grating cycle as abscissa. For the non-random arrangement of dots this number is the number of dots per grating cycle along any vertical column of dots at right angles to the horizontal bars of the grating. For the quasi-random arrangement of dots the number is the mean number along a line at right angles to the bars.

Fig. 2A and B shows that discrimination threshold fell to an asymptotic value when the number of dots per grating cycle exceeded ≈3. Threshold rose steeply when the number of dots per cycle was reduced below 3, and the rise was steeper for the non-random arrangement then for the quasi-random arrangement.

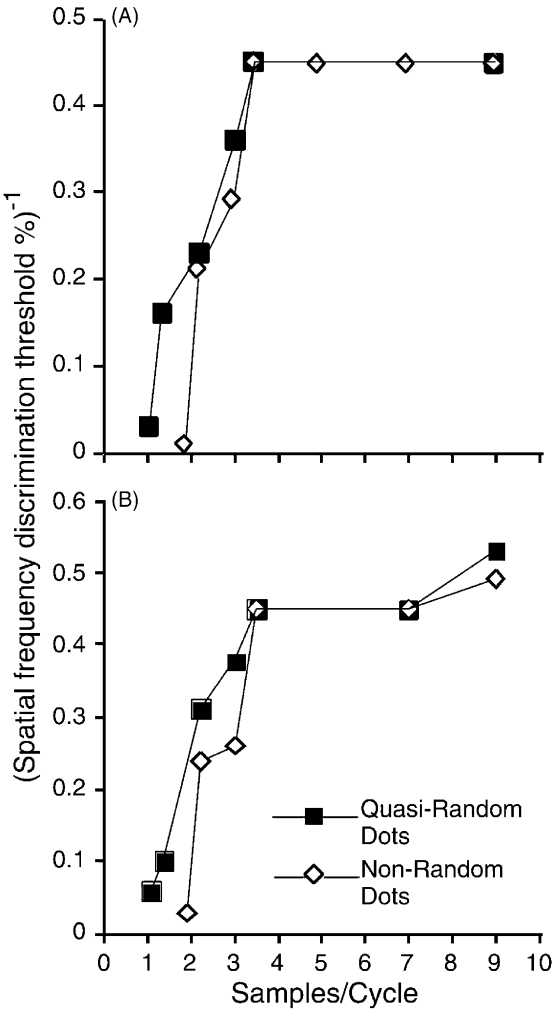

Fig. 2. The reciprocal of spatial frequency discrimination threshold for a cyclopean grating was plotted as ordinate versus the number of dots per grating cycle along a line at right angles to the bars of the grating. The dots were arranged either quasi-randomly or non-randomly. Standard error bars were smaller than the symbols. A: Observer 1 and B: Observer 4.

3.5. Discussion

When the non-random dot pattern was used, the discrimination task became essentially impossible when the number of samples per cycle fell below two. (This was because the number of samples per cycle was varied independently of spatial frequency. Had this not been done, measured sensitivity to differences of spatial frequency would not have fallen to near-zero at two samples per cycle, because a reliable—though spurious—cue to the discrimination task would have been provided by depth corrugations caused by interactions between the grating's nominal spatial frequency and the number of samples per cycle.)

Our proposed explanation for the difference between the curves for non-random and quasi-random dot patterns is as follows. Even if the visual system integrated information parallel to the grating's bars no further sampling information would have been provided in the non-random case because the horizontal rows of dots were parallel to the bars. In contrast, spatial integration parallel to the bars would, in effect, increase the number of samples per grating cycle in the quasi-random case. The data shown in Fig. 2A and B allow us to estimate the spatial extent of integration. Sensitivity to differences in spatial frequency fell to zero at ≈1.0 samples per cycle in the quasi-random case and at ≈1.9 samples per cycle in non-random case, indicating that the spatial integration along the bars renders one sample per cycle in the quasi-random case effectively equal to ≈1.9 samples per cycle. Given that the mean horizontal distance between dots was 1.56° when the number of samples per cycle was 1.0, we concluded that the cyclopean visual system integrates over a distance of ≈1.6° along the length of a depth corrugation. The advantage given by this spatial integration diminishes progressively as the number of

samples per cycle is increased beyond 1 until, at three samples per cycle, no advantage remained.

We conclude that cyclopean gratings should contain at least three dots per grating cycle along a line perpendicular to the bars. [3]

4. Experiment 2

4.1. Purpose

The aim of Experiment 2 was to compare discrimination threshold for the periodicity of depth corrugations in a cyclopean grating with discrimination threshold for the periodicity of luminance modulation in a luminance-defined grating of matched spatial sampling.

4.2. Observers

Observers 1 and 2 participated in Experiment 2.

4.3. Methods

Each eye saw a mean number of 7100 dots. The display was masked to subtend 15° (horizontally) × 12° at a viewing distance of 114 cm. A complete stereo pair was presented every 29 ms. Dots were arranged quasi-randomly.

To avoid undue spread of power in the frequency spectrum the lowest number of cycles in the display was 5. (In this situation power fell to half of its maximum value at spatial frequencies ±20% to either side of the nominal spatial frequency, see Regen (2000, pp. 418–420)). Measurements were made in the following conditions: viewing distance 57 cm, five cycles displayed; viewing distance 114 cm, either five or nine cycles displayed; viewing distance 228 cm, nine cycles displayed. This gave a spatial frequency range of 0.16–2.0 cycles/°. Beyond the highest spatial frequency (2 cycles/°) the visibility of the cyclopean grating fell sharply.

The mean disparity of the cyclopean grating was zero, and peak-to-trough disparity was 4.2′. The mean disparity of the luminance-defined grating was zero, and the luminance contrast was varied between 70% and 95%.

4.4. Results

Set of curves similar to Fig. 1A and D were obtained for both cyclopean and luminance-defined gratings. In every case the curves showed that observers based their responses entirely on the task-relevant variable. Fig. 3A and B compares sensitivity to a difference in the periodicity of depth corrugations (open symbols) with sensitivity to the periodicity of luminance modulation (filled

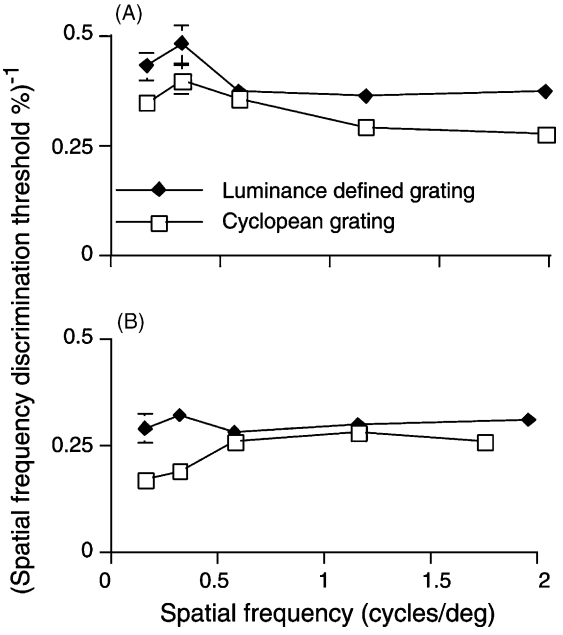

Fig. 3. The reciprocal of spatial frequency discrimination threshold was plotted as ordinate for cyclopean (open symbols) and luminance-defined (filled symbols) gratings versus grating spatial frequency. A: Observer 1 and B: Observer 2.

[3] According to Nyquist's theorem, sufficient information to reproduce a continuous waveform that is band-limited to B Hz can be obtained by recording independent samples of the waveform (periodically or aperiodically) at a rate just $>B$ times per second. Alternatively, a signal of duration T (in seconds) can be specified completely by just more than $2BT$ independent samples of the signal. The sampling process introduces frequency components not present in the original waveform, so that to recover the original signal the sampled signal must be passed through an 'ideal filter' that totally removes all frequencies above B Hz while having no effect on all frequencies below B Hz. However, an 'ideal filter' is a mathematical artifact. Since realizable filters fall short of this ideal, sampling frequencies considerably above B Hz are used in human-made devices. If the sampling rate is less than B Hz, the recovered low-pass filtered signal will contain frequency components not present in the original signal. This effect is called aliasing (Schwartz, 1970). The physiological approximation to an 'ideal filter' is likely to be far from ideal. The frequency content of a long sinusoidal waveform is narrowly centered on P^{-1} Hz (where P is the frequency of the sinusoid in seconds). The act of restricting the sinusoid to a few cycles broadens its power spectrum, so that power can extend to frequencies considerably $> P^{-1}$. Consequently for a windowed sinusoid the Nyquist frequency is higher than P^{-1}.

Although originally framed in terms of the time/temporal frequency domains, sampling theory can be extended to the space/spatial frequency domains. In our present case, the cyclopean equivalent of an 'ideal filter' is likely to be far from ideal. This, combined with the windowing effect just mentioned would extend the degradation of cyclopean vision to sampling rates above the nominal Nyquist frequency of $2P^{-1}$. Appendix F in Regan (2000, pp. 467–481) provides a more complete discussion of sampling in the context of both the stimulus and of retinal processing.

symbols) as a function of the spatial frequency of the grating. Except where shown, standard errors were smaller than the symbols. For observer 1 (Fig. 1A) and 2 (Fig. 1B) sensitivity was almost independent of grating spatial frequency over the range 0.16–2.0 cycles/°. This was the case for both cyclopean and luminance-defined gratings. At every spatial frequency tested, discrimination threshold was lower for the luminance grating than for the cyclopean grating, though the difference was only slight. This was the case for both observers.

For observer 1 the lowest value of spatial frequency discrimination threshold was 2.5% for the cyclopean grating and 2.1% for the luminance-defined grating. Corresponding thresholds for observer 2 were 3.5% and 3.1%.

4.5. Discussion

We conclude that spatial frequency discrimination threshold is only slightly higher for a cyclopean grating than for a luminance-defined grating of matched sampling. Cyclopean discrimination thresholds were considerably lower than the psychophysically-estimated spatial frequency bandwidth of cyclopean channels, or of channels for luminance-defined form (Graham, 1989) or of the most sharply-tuned neurons in monkey striate cortex (DeValois, Albrecht, & Thorell, 1982).

We suggest that this discrepancy can be explained by analogy with the corresponding discrepancy for luminance-defined form (Campbell, Nachmias, & Jukes, 1970; Regan & Beverley, 1983; Regan, Bartol, Murray, & Beverley, 1982). In particular, we propose that discrimination threshold for cyclopean gratings is determined by the pattern of activity among cyclopean channels that prefer different spatial frequencies. In Experiment 4 we will subject this hypothesis to experimental test.

5. Experiment 3

5.1. Purpose

The purpose of Experiment 3 was to find how spatial frequency discrimination threshold for a cyclopean grating was affected by the peak-to-trough disparity of the grating.

5.2. Observers

Observers 1 and 3 participated in Experiment 3.

5.3. Methods

From the viewing distance of 228 cm the display subtended 7.7° (horizontal) × 7.7°. There were nine cycles across the display, so that the spatial frequency was 1.16 cycles/°. Each eye saw a mean number of 7100 dots. A complete stereopair was presented every 29 ms. Discrimination thresholds were measured over a ≈500:1 range of peak-to-trough disparities from 0.1 to 49′. The procedure in the main experiment was as described in General Methods.

In a subsidiary experiment we measured grating detection threshold. The stimulus set contained two values of peak-to-trough disparity, namely zero and a value that gave a d' near 1.0. For each value of peak-to-trough disparity there were eight values of spatial phase, giving 16 stimuli in all. Observers were instructed to signal which of the two possible values of peak-to-trough disparity had just been presented. The value of d' was calculated conventionally (Macmillan & Creelman, 1991).

5.4. Results

Grating detection threshold ($d' = 1.0$) for observer 1 was estimated as 0.18′ peak-to-trough and, for observer 3, 0.41′ peak-to-trough. Fig. 4A and B shows that, as the peak-to-trough disparity was progressively increased above grating detection threshold, spatial frequency discrimination threshold fell steeply to ≈1.7% for observer 1 (4.4% for observer 3), and thereafter remained approximately independent of peak-to-trough disparity over a range of ≈45:1 for observer 1 and ≈17:1 for observer 3. Binocular fusion became difficult when peak-to-trough disparity was increased further, and discrimination threshold rose correspondingly.

5.5. Discussion

It is not surprising that spatial frequency discrimination threshold rose sharply when the peak-to-trough disparity approached grating detection threshold nor when peak-to-trough disparity was so large that it rendered binocular fusion intermittent: one would expect that the curves in Fig. 4A and B would have the shape of an inverted U. The interesting aspect of Fig. 4A and B is the 45:1 and 17:1 ranges over which discrimination threshold is approximately independent of peak-to-trough disparity. It has previously been reported the spatial frequency discrimination threshold for luminance-defined form (and also orientation discrimination threshold and line separation threshold) are approximately independent of luminance contrast over a similarly wide range of contrasts (Morgan & Regan, 1987; Regan and Beverley, 1983, 1985; Regan et al., 1982; Skottun, Bradley, Sclar, Ohzawa, & Freeman, 1987). The explanation proposed for these findings was that the discrimination thresholds were determined by the pattern of activation among tuned neurons, possibly by opponent-processing as discussed mathematically in the

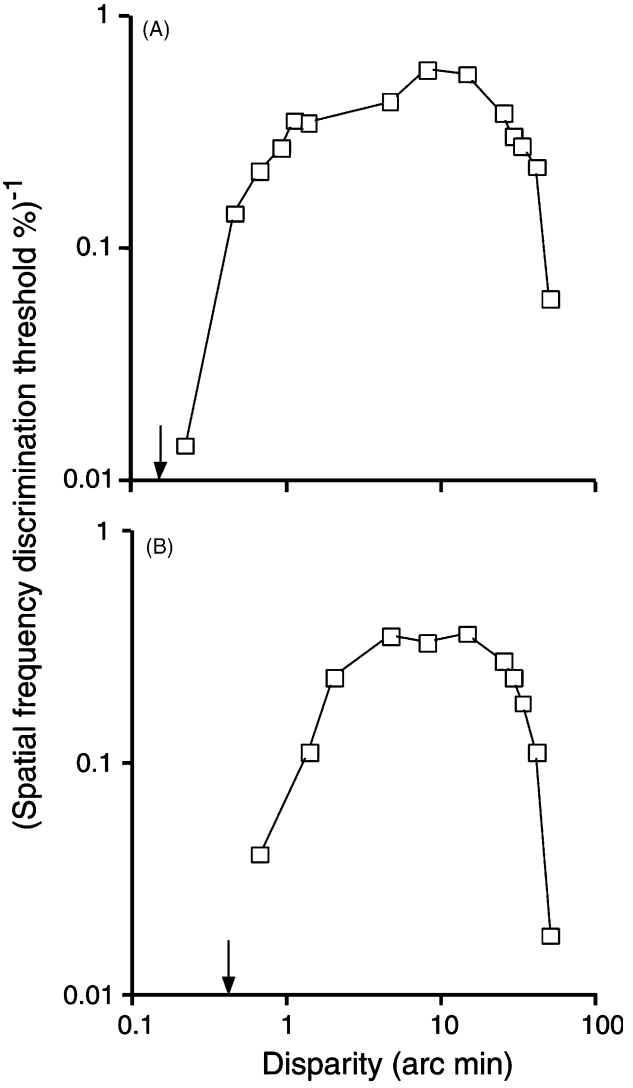

Fig. 4. The reciprocal of spatial frequency discrimination threshold for a cyclopean grating was plotted as ordinate versus the peak-to-trough disparity of the grating. Note that both axes are logarithmic. Grating detection thresholds are arrowed. The dots were arranged quasi-randomly. Standard error bars were smaller than the symbols. A: Observer 1 and B: Observer 3.

appendix in Morgan and Regan (1987) and Regan and Beverley (1985). We suggest that the approximately flat regions in Fig. 4A and B can be explained analogously, and will test this hypothesis in Experiment 4.

6. Experiment 4

6.1. Purpose

The purpose of Experiment 4 was to test the hypothesis that spatial frequency discrimination threshold for cyclopean gratings is determined by the pattern of activity among cyclopean neurons tuned to spatial frequency. Our procedure was to compare the effects of adaptation on spatial frequency discrimination threshold and on grating detection threshold (Regan, 1982; Regan & Beverley, 1983, 1985; Regan et al., 1982).

6.2. Methods

From the viewing distance of 114 cm the display subtended 15° (horizontally) × 15°. Each eye saw a mean number of 7100 dots. A complete stereopair was displayed every 29 ms.

After viewing a cyclopean adapting grating for 5 min, a cyclopean test grating was presented, followed by a 10 s refresh of adaptation, followed by another test presentation, and so on. Test presentation duration was 400 ms for observer 1 and 600 ms for observer 4. Adaptation, refresh and test gratings all had zero mean disparity and 4.2′ peak-to-trough disparity. An adapt/refresh grating had one of eight equally-spaced spatial phases, and switched to a randomly-selected phase every 500 ms. The phase of a test grating was selected randomly from the eight possibilities. When measuring the effect of adaptation on spatial frequency discrimination, the test grating had one of two possible spatial frequencies that differed by 3.75%, each spatial frequency being paired with eight spatial phases, giving 16 test stimuli in all. Following each presentation of a test grating, observers were instructed to signal whether the spatial frequency was high or low, and d' estimates were made conventionally (Macmillan & Creelman, 1991). Baseline values of d' were obtained using the same procedure except that the adapting grating had a peak-to-peak disparity of zero.

Baseline and postadaptation values of d' for detecting the grating were measured by combining the adaptation/refresh procedure just described with the test procedure used in Experiment 3 with a 400 ms (observer 1) or 600 ms (observer 2) test presentation duration.

6.3. Observers

Observers 1 and 4 carried out Experiment 4.

6.4. Results

The ratio (baseline d')/(postadaptation d') was plotted as ordinate in Fig. 5A and B versus the test spatial frequency as abscissa. Open symbols in Fig. 5A confirm the previous finding (Schumer & Ganz, 1979) that, after inspecting a high-visibility cyclopean grating, detection threshold for a test grating is elevated maximally at the adapting spatial frequency, and that the detection threshold elevation falls off as the difference between the spatial frequencies of the test and adapting gratings is increased.

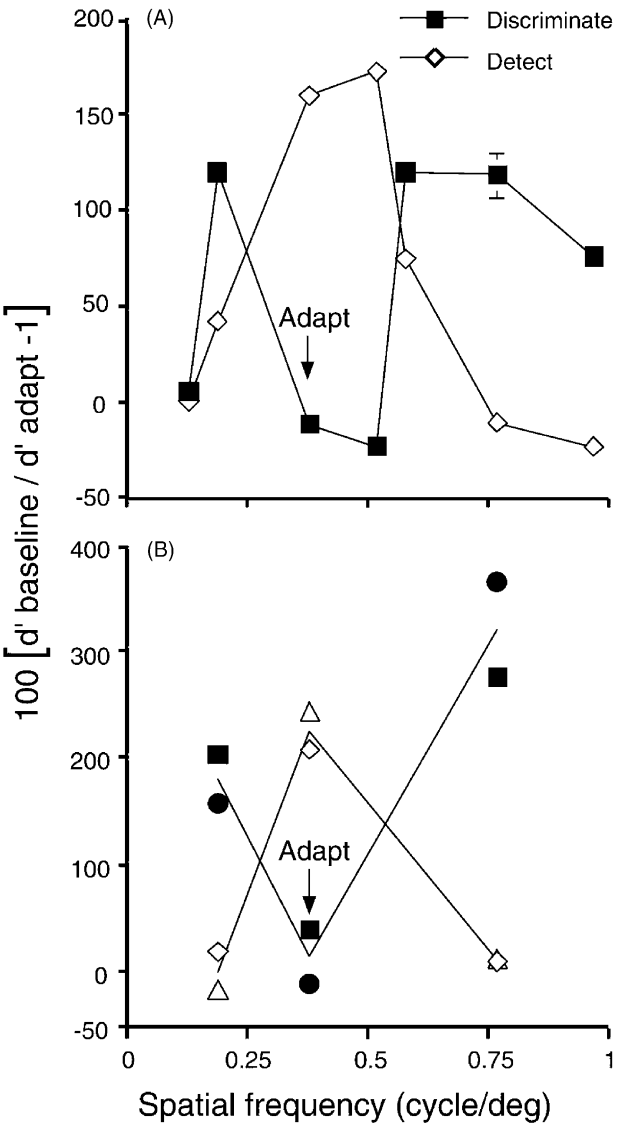

Fig. 5. The effect of adapting to a cyclopean grating on grating detection threshold (open symbols) and spatial frequency discrimination threshold (filled symbols) for cyclopean test gratings. The ratio (baseline d')/(postadaptation d') was plotted as ordinate versus the spatial frequency of the test grating. Vertical arrows mark the spatial frequency of the adapting grating. A: Observer 1 and B: Observer 4.

Our main finding is that adaptation produced the opposite effect on spatial frequency discrimination threshold. Filled symbols in Fig. 5A and B show that discrimination threshold was, if anything, slightly improved at the adapting spatial frequency for observer 1 and unaffected for observer 4. The maximum post-adaptation elevation of discrimination threshold occurred at test frequencies offset from the adapting frequency, where detection threshold was comparatively unaffected by adaptation. In Fig. 5A the data plotted as filled symbols second and fifth from the right were subjected to a two-tailed t-test. The difference was highly significant ($t = -6.26$, df $= 4$, $p = 0.003$).

6.5. Discussion

The finding that grating detection threshold is elevated maximally at the adapting spatial frequency is conventionally taken to indicate that the most highly activated spatial frequency channel determines detection threshold (Graham, 1989). Our data can be understood if spatial frequency discrimination threshold is determined by comparatively weakly-activated channels.

Filled symbols in Fig. 5A and B indicate that the effect of activation of the most sensitive channel was, if anything, deleterious to spatial frequency discrimination. As noted earlier (Regan & Beverley, 1983, 1985), slight post-adaptation reduction in discrimination threshold at the adapting frequency would be expected if random noise from the channel most sensitive to the test grating reduces the signal-to-noise ratio of the "frequency change" signal.

Following a previous argument (Regan & Beverley, 1983) and referring to Fig. 6, we assume that a small change of test spatial frequency from S_1 to S_2 traverses the almost-flat top of the most sensitive cyclopean channel (b) so that the output of this channel changes negligibly. The two most important cyclopean channels for spatial frequency discrimination, a and c, are those whose slopes differ most at the test frequency. It follows that, as shown in Fig. 5A and B, the maximum effect of adaptation on discrimination threshold will be at frequencies offset from the adapting frequency. By analogy with our previous discussion of spatial frequency discrimination for luminance-defined form

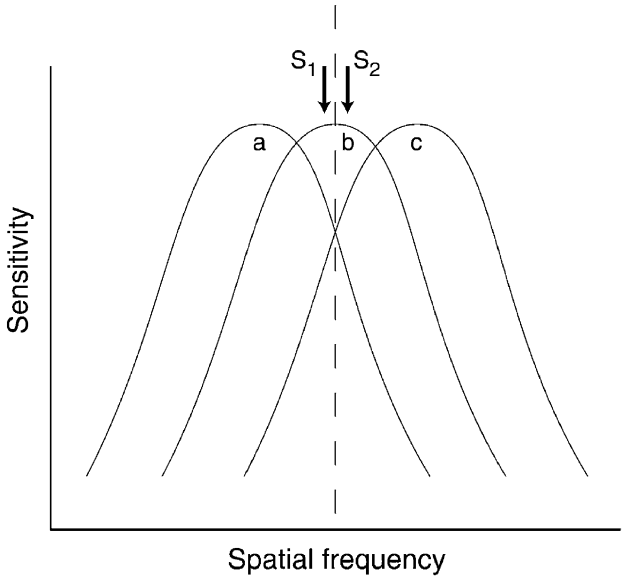

Fig. 6. Proposed explanation for the postadaptation data of Fig. 5. A small change of test spatial frequency from S_1 to S_2 produces little change in the output of the cyclopean filter (b) that is most sensitive to the cyclopean test grating, but produces a large change in the balance between the outputs of the offset filters a and c.

(Regan & Beverley, 1983), the hypothesis that spatial frequency discrimination threshold for cyclopean gratings is determined by the relative activity among cyclopean channels (we suggest by an opponent process) can, as discussed earlier, account for the findings that (1) discrimination threshold is far lower than the estimated bandwidth of cyclopean channels (Fig. 3) and (2) that discrimination threshold is approximately constant over a wide range of peak-to-peak disparities (Fig. 4).

Acknowledgements

We are grateful to Dr. X.H. Hong for writing the software for this study. We thank Derek Harnanan Singh., Nucci Lein Villareal and Nancy Cowell for their patience as observers. This research was supported by the Natural Sciences and Engineering Council of Canada (NSERC operating grant to DR). DR holds the NSERC/CAE Industrial Research Chair in Vision and Aviation. Effort sponsored by the Air Force Office of Science Research, Air Force Material Command, USAF, under grant number F49620-00-1-0053. The US Government is authorized to reproduce and distribute reprints for governmental purposes notwithstanding any copyright violation thereon. The views and conclusions contained herein are those of the authors and should not be interpreted as necessarily representing the official policies or endorsements, either expressed or implied, of the Air Force Office of Scientific Research or of the US Government.

References

Campbell, F. W., & Robson, J. G. (1968). Application of Fourier analysis to the visibility of grating. *Journal of Physiology, 197*, 551–566.

Campbell, F. W., Nachmias, J., & Jukes, J. (1970). Spatial frequency discrimination in human vision. *Journal of the Optical Society of America, 60*, 555–559.

Cavanagh, P. (1989). Multiple analyses of orientation in the visual system. In D. Lam (Ed.), *Neural mechanisms of visual perception* (pp. 25–43). The Woodlands, TX: Portfolio Publishing.

Cobo-Lewis, A. B., & Yeh, Y. Y. (1994). Selectivity of cyclopean masking for spatial frequency of binocular disparity modulation. *Vision Research, 34*, 607–620.

DeValois, R. L., Albrecht, D. G., & Thorell, L. G. (1982). Spatial frequency selectivity of cells in macaque visual cortex. *Vision Research, 22*, 545–559.

Finney, D. J. (1971). *Probit analysis*. Cambridge: Cambridge University Press.

Graham, N., & Nachmias, J. (1971). Detection of grating patterns containing two spatial frequencies: A comparison of single-channel and multiple-channel models. *Vision Research, 11*, 251–259.

Graham, N. (1989). *Visual pattern analyzers*. New York: Oxford University Press.

Hamstra, S. J., & Regan, D. (1995). Orientation discrimination in cyclopean vision. *Vision Research, 35*, 365–374.

Howard, I. P., & Rogers, B. J. (1995). *Binocular vision and stereopsis*. New York: Oxford University Press.

Julesz, B. (1960). Binocular depth perception of computer-generated patterns. *Bell System Technical Journal, 39*, 1125–1162.

Julesz, (1971). *Foundations of cyclopean perception*. Chicago: University of Chicago Press.

Julesz, B., & Miller, J. E. (1975). Independent spatial-frequency-tuned channels in binocular fusion and rivalry. *Perception, 4*, 125, 143.

Kohly, R. P., & Regan, D. (2001). Long-distance interactions in cyclopean vision. *Proceedings of the Royal Society, 268*, 213–219.

Macmillan, N. A., & Creelman, C. D. (1991). *Detection theory: a user's guide*. Cambridge: Cambridge University Press.

Morgan, M. J. (1986). Positional acuity without monocular cues. *Perception, 15*, 157–162.

Morgan, M. J., & Regan, D. (1987). Opponent model for line interval discrimination: Interval and vernier performance compared. *Vision Research, 27*, 107–118.

Regan, D. (1982). Visual information channeling in normal and disordered vision. *Psychological Review, 89*, 407–444.

Regan, D. (2000). *Human perception of objects: early processing of spatial form defined by luminance, color, texture, motion, and binocular disparity*. Sunderland, MA: Sinauer.

Regan, D., & Beverley, K. I. (1983). Spatial frequency discrimination and detection: comparison of postadaptation thresholds. *Journal of the Optical Society of America, 73*, 1684–1690.

Regan, D., & Beverley, K. I. (1985). Postadaptation orientation discrimination. *Journal of the Optical Society of America, 2*, 147–155.

Regan, D., & Hamstra, S. J. (1994). Shape discrimination for rectangles defined by disparity alone, disparity plus luminance and by disparity plus motion. *Vision Research, 34*, 2277–2291.

Regan, D., Bartol, S., Murray, T. J., & Beverley, K. I. (1982). Spatial frequency discrimination in normal vision and in patients with multiple sclerosis. *Brain, 105*, 735–754.

Rogers, B. J., & Graham, M. E. (1985). Motion parallax and the perception of threedimensional surfaces. In D. Ingle, M. Jeannerod, & D. Lee (Eds.), *Brain mechanisms and spatial vision* (pp. 95–111). The Hague: Martinus Nijhoff.

Schumer, R. A., & Ganz, L. (1979). Independent stereoscopic channels for different extents of spatial pooling. *Vision Research, 19*, 1303–1314.

Schwartz (1970). *Information transmission, modulation and noise*. New York: McGraw-Hill.

Skottun, B. C., Bradley, A., Sclar, G., Ohzawa, I., & Freeman, R. D. (1987). The effect of contrast on visual orientation and spatial frequency discrimination: A comparison of single cells and behaviour. *Journal of Neurophysiology, 57*, 733–786.

Smallman, H. S., MacLeod, D. T. A., He, S., & Kentridge, R. W. (1996). Fine grain of the neural representation of human spatial vision. *Journal of Neuroscience, 16*, 1852–1859.

Tyler, C. W. (1974). Depth perception in disparity gratings. *Nature, 251*, 140–142.

Tyler, C. W. (1975). Stereoscopic tilt and size aftereffects. *Perception, 4*, 187–309.

Tyler, C. W. (1983). Sensory processing of binocular disparity. In C. M. Schor, & K. J. Cuiffreda (Eds.), *Vergence eye movements* (pp. 199–295). Boston, MA: Butterworth.

Wheatstone, C. (1838). Contributions to the physiology of vision. *Philosophical Transactions of the Royal Society, 13*, 371–394.